Land Degradation & Development

WILEY

RESEARCH ARTICLE

Accelerated Decline in Vegetation Resilience on the Tibetan Plateau

Yantao Liu[1] | Pengfeng Xiao[1,2,3] | Xueliang Zhang[1,2] | Hao Liu[1] | Siyong Chen[1] | Yumeng Jia[1]

[1]Jiangsu Provincial Key Laboratory of Geographic Information Science and Technology, Key Laboratory for Land Satellite Remote Sensing Applications of Ministry of Natural Resources, School of Geography and Ocean Science, Nanjing University, Nanjing, Jiangsu, China | [2]Frontiers Science Center for Critical Earth Material Cycling, Nanjing University, Nanjing, Jiangsu, China | [3]Jiangsu Center for Collaborative Innovation in Geographical Information Resource Development and Application, Nanjing, Jiangsu, China

Correspondence: Pengfeng Xiao (xiaopf@nju.edu.cn)

Received: 1 July 2024 | **Revised:** 3 October 2024 | **Accepted:** 13 October 2024

Funding: This work was supported by National Natural Science Foundation of China (Grant No. 42171307) and the "GeoX" Interdisciplinary Research Funds for the Frontiers Science Center for Critical Earth Material Cycling, Nanjing University.

Keywords: critical slowing down | NIRv | Tibetan Plateau | vegetation resilience

ABSTRACT

The ability of ecosystems to resist and recover from external disturbances is declining due to climate change, increased frequency of disasters, and intensified human activities. Global vegetation resilience is considered to be at risk of being lost. The sensitive and fragile Tibetan Plateau (TP) has experienced changes in climate and management patterns over the past five decades, but due to the complexity of defining resilience, there is still no unified understanding of the spatial patterns and long time-series trends of resilience on the TP. In this study, we introduce the method based on critical slowing down, making it possible to clarify the spatial distribution and temporal dynamics of resilience on the TP. The results show low resilience on the northeastern and southwestern edges of the TP and in the Three River Source region. The area experiencing resilience loss is approximately 1.16–1.44 times larger than the area of gain. Vegetation resilience on the TP has exhibited a declining trend, with the rate of decline after 2014 being more than double that of the preceding period. Factors such as elevation, vegetation type, and hydrothermal condition significantly influence the spatial and temporal patterns of resilience. These findings improve our understanding of vegetation resilience on the TP and its ecosystem vulnerability. We also recommend that ecological restoration efforts be maintained and regularly assessed.

1 | Introduction

The Tibetan Plateau (TP) has experienced rapid warming (Chen et al. 2013), shifting precipitation patterns (Yao et al. 2019), and overgrazing (Zhu et al. 2023) over the past five decades. As a result of these factors, the TP faces the loss of species richness and diversity (Piao et al. 2019), reduced soil erodibility (Lin et al. 2023), and severe grassland degradation (Liu et al. 2018), with a risk of further deterioration in the future (Pan et al. 2018; Zhu et al. 2023). Given these unfavorable ecological risks and increasingly frequent disturbances (Zhang et al. 2023), the vegetation resilience—the ability to resist an external perturbation and not switch to another state, and the speed of recovery after a perturbation (Dakos and Kéfi 2022; Willis, Jeffers, and Tovar 2018)—has received widespread attention (Fang and Zhang 2019; Gao et al. 2019; Li, Wu, et al. 2020; Lu et al. 2023).

Some studies have analyzed the process of vegetation restoration (An et al. 2021; Zhang et al. 2015), mechanisms of vegetation recovery (Fang and Zhang 2019; Lu et al. 2023; Yin et al. 2024), and ecological restoration management (Ji et al. 2024; Xu and Grumbine 2014) on the TP; however, the spatial patterns and

long-term trends of resilience on the TP remain unclear. While there are studies on these spatial patterns, their conclusions are not entirely consistent. For instance, one study indicates that the areas of low resilience on the TP are located in the Western Himalayas and in the southeastern Qilian Mountains (Li, Wu, et al. 2020). Another study suggests that the Three River Source region also has low resilience (Li, Zhang, et al. 2020). While another study posits that resilience is generally high on the eastern TP, particularly in the Qilian Mountains, where it is even the highest (Li et al. 2021). These contradictions arise because resilience in these studies is defined by different types of disturbances, and the ecosystem's ability to recover from climate change and human activities cannot evaluated on the same dimension.

There are few studies on the long-term trends of resilience on the TP, primarily due to methodological constraints (Teng et al. 2020). There are three methods of quantifying resilience trends: the first approach assesses changes in recovery rates following historical disturbances (Fang and Zhang 2019; Fu et al. 2020; Gao et al. 2024; Lu et al. 2023). Evidence from tree rings suggests that the resilience of trees to drought events has increased over the past 50 years (Fang and Zhang 2019). This method is effective when studying specific species or disturbance events, but pulsed disturbances and recoveries may not form a continuous time series. The second approach involves aggregated indicators (Teng et al. 2020; Xia et al. 2021). One assessment shows that the resilience of the plant–soil system in alpine meadows tends to increase with recovery time (Gao et al. 2019), and another system suggests that resilience in the eastern TP also shows fluctuating increases (Ji et al. 2024). This method is well-suited for assessing continuous changes in resilience, but the unified system of resilience indicators needs more validation (Gao et al. 2019). The third approach estimates resilience from vegetation change characteristics, with the ARx model being the most commonly used (Li, Wu, et al. 2020; Li, Zhang, et al. 2020; Yang et al. 2022). The model indicates that resilience on the TP slightly declined after 2008 compared to the period before 2008 (Yang et al. 2022). This method overcomes the limitations of vegetation types and disturbances and is more objective than indicator-based evaluations. However, there are still uncertainties associated with the accuracy of temperature or drought data, and errors in function fitting (De Keersmaecker et al. 2015). These limitations lead to unclear spatial and temporal patterns of resilience on the TP.

Recently, a remote sensing method based on critical slowing down has provided a new perspective (Smith and Boers 2023a; Smith, Traxl, and Boers 2022; Verbesselt et al. 2016). When the ecosystem is assumed to be multistable, disturbances will cause it to deviate from current state and resilience will return it to stability. Thus the system does not usually reach the tipping point of multistability leading to catastrophic shift (Dakos and Kéfi 2022; Scheffer et al. 2001). Critical slowing down refers to the phenomenon where, as a system approaches a tipping point, the time required to return to equilibrium increases, indicating a reduction in resilience (Scheffer et al. 2009). This usually manifested by increases in variance and first-order autocorrelation (AC1) (Boulton, Lenton, and Boers 2022; Forzieri et al. 2022; Hu et al. 2023). This method, which estimates resilience from intrinsic ecosystem changes using only vegetation metrics, has already been applied and validated globally (Smith, Traxl, and Boers 2022; Yao, Liu, Fu, et al. 2024) and in several key regions (Boulton, Lenton, and Boers 2022; Wang et al. 2023). This made it possible to conduct long time series and large-scale studies of resilience. A recent study showed that the accuracy of resilience estimation is heavily influenced by the choice of vegetation metrics (Smith and Boers 2023b). It is critical to identify the region-specific vegetation metric (Bathiany et al. 2024), but this is currently unclear on the TP.

To tackle the aforementioned challenges, we first evaluated nine metrics and employed three data synthesis methods to identify the most reliable metric for estimating resilience on the TP. Vegetation resilience trends and spatial patterns at the pixel level were then quantitatively analyzed for various periods and subregions using the best performing metric. We aim to address two key questions: (1) which metric serves as a superior estimator of vegetation resilience on the TP and (2) what are the spatial patterns of vegetation resilience and the trends over the past two decades on the TP? This work aids in reassessing the health of the TP ecosystem and plays a crucial role in guiding ecosystem conservation and restoration endeavors, particularly as integral components of nature-based solutions.

2 | Materials and Methods

2.1 | Study Area

The TP (25°59′–40°00′ N, 73°20′–104°47′ E) is the highest plateau in the world, covering an area of approximately $2.5 \times 10^6\,km^2$ and an average altitude more than 4000 m (Figure 1) (Liu et al. 2023). Renowned as the "Asian Water Tower," the TP exerts profound influences on both local and distant ecosystems through its streamflow (Chen et al. 2023) and moisture recycling (Li et al. 2023), serving as a vital ecological barrier. Due to its low latitude and high elevation, the TP has strong solar radiation, uneven precipitation, and low average temperatures. Differences in natural conditions on the TP lead to large variations in hydrological conditions (Liu et al. 2023), the richness of vegetation types, and a significant carbon repository (Wei et al. 2021), making it an ideal laboratory to study resilience in different scenarios.

2.2 | Methods

2.2.1 | Data Sources and Preprocessing

A recent study has shown that using single-sensor satellite data can reduce errors caused by the signal-to-noise ratio of cross-sensor data (Smith et al. 2023). Therefore, nine commonly used vegetation metrics, primarily sourced from the Moderate-resolution Imaging Spectroradiometer (MODIS) from February 2000 to December 2022, were employed to estimate resilience. NDVI and EVI were derived from the MOD13Q1 dataset. kNDVI is a nonlinear extension of NDVI (Camps-Valls et al. 2021), exhibiting antisaturation and stable characteristics. Leaf area

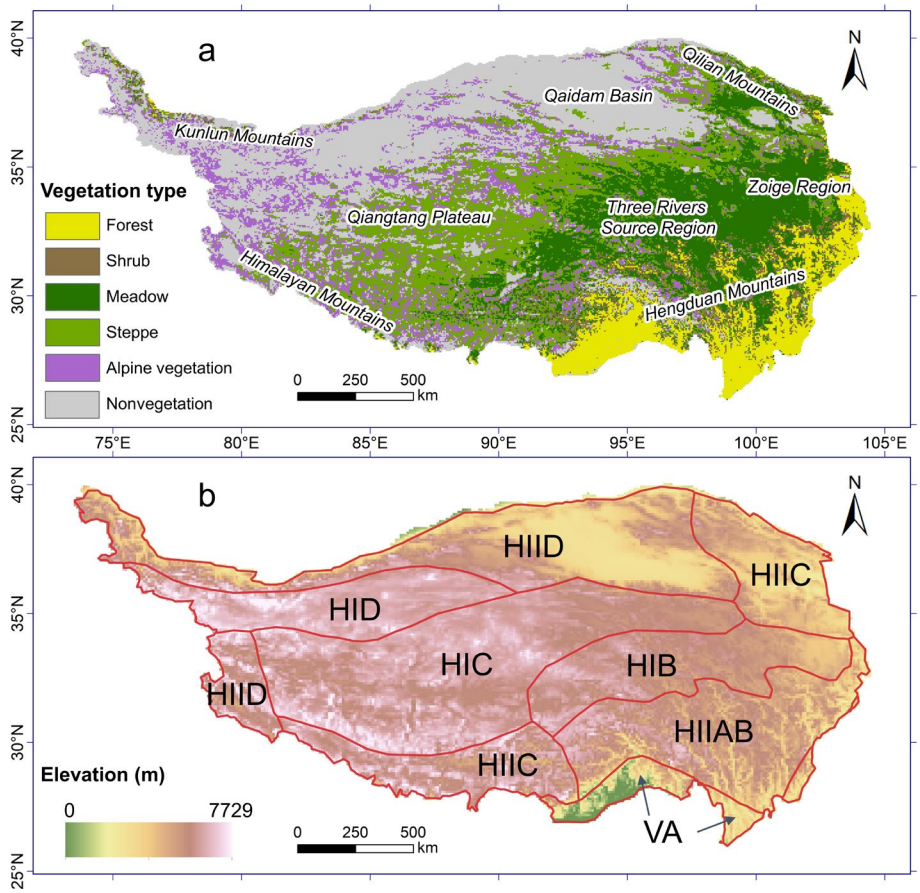

FIGURE 1 | Vegetation types (Zhou et al. 2023) (a) and elevation with eco-geographic regions (Wu, Yang, and Zheng 2003) (b) of the Tibetan Plateau. The full names of the eco-geographic regions can be found in Table S1. [Colour figure can be viewed at wileyonlinelibrary.com]

index (LAI) was derived from MCD15A3H and gross primary productivity (GPP) from MOD17A2H. NIRv is the product of NIR reflectance and NDVI (Badgley, Field, and Berry 2017), calculated based on MCD43A4. We used the vegetation optical depth (VOD) dataset, which characterizes the water content of vegetation (Sawada et al. 2016) and has been widely used in resilience estimation studies (Boulton, Lenton, and Boers 2022; Smith, Traxl, and Boers 2022). Solar-induced chlorophyll fluorescence (SIF) was proposed as a proxy for vegetation photosynthesis and was also incorporated. Two types of SIF data, GOSIF (Li and Xiao 2019) and RTSIF (Chen et al. 2022), were employed in this study. The vegetation types were obtained from (Zhou et al. 2023), with an overall accuracy of 89.5% and a Kappa coefficient of 0.87 for the TP.

All datasets followed a standardized preprocessing procedure. Specifically, we firstly filtered out pixels with a maximum NDVI over 20 years less than 0.1, which are considered negligible vegetation cover (Zhang et al. 2013). Second, we eliminated pixels where vegetation types had undergone shifts during the study period, thereby excluding disturbances stemming from community succession. Given the disparate temporal resolutions of the various datasets, we normalized the data to monthly values employing three synthesis methods: maximum, median, and mean. To address potential missing values, we employed a harmonic fitting method. Finally, we resampled the data to 0.05° to accommodate the different resolutions. All data acquisition and preprocessing tasks were implemented in Google Earth Engine (Gorelick et al. 2017).

2.2.2 | Estimating Vegetation Resilience

Estimating continuous resilience from vegetation metric time series requires following steps. First, it is necessary to eliminate trends and seasonality from the original time series. We employed seasonal-trend decomposition using loess (STL), which is an effective and widely used model that can separate the residuals from the seasonality and trend of time series (Verbesselt et al. 2016). Second, for the residual time series, we separately calculated the AC1 and variance, which are considered proxy indicators of vegetation resilience (Smith, Traxl, and Boers 2022; Verbesselt et al. 2016; Wang et al. 2023):

$$\mathrm{ac1} = \frac{\sum_{t=1}^{N-1}\left(x_t-\bar{x}\right)\left(x_{t+1}-\bar{x}\right)}{\sqrt{\sum_{t=1}^{N}\left(x_t-\bar{x}\right)^2 \times \sum_{t=1}^{N-1}\left(x_{t+1}-\bar{x}\right)^2}} \quad (1)$$

$$v = \frac{1}{N-1}\sum_{t=1}^{N}\left(x_t-\bar{x}\right)^2 \quad (2)$$

where ac1 and v represent the AC1 and variance, respectively; N represents the time window size, set to 60 months in this study; x represents the residual series of vegetation metrics and

$\overline{x}$ represents the mean of the residual series within the window. Smaller AC1 and variance values signify faster system recovery and less deviation from the equilibrium state.

Although AC1 and variance are correlated with resilience, they are not equivalent to resilience (Dakos et al. 2012). Therefore, thirdly, we calculate the theoretical value of resilience based on the functional relationship between the proxies (AC1 and variance) and recovery rate proved by (Smith and Boers 2023b):

$$r_{ac1} = \frac{1}{\Delta t}\log(ac1) \tag{3}$$

$$r_v = \frac{1}{2\Delta t}\log\left(1 - \frac{\overline{\sigma}^2}{v}\right) \approx -\frac{\overline{\sigma}^2}{2v\Delta t} \tag{4}$$

where r_* represents resilience estimated using proxies; Δt represents the discrete step size, set to 1 in this study; the noise $\overline{\sigma}$ can be obtained by regression on the discrete data:

$$\overline{\sigma} = \sqrt{\frac{1}{N-1}\sum_{t=1}^{N-1}\left(\frac{\Delta x}{\Delta t} - \lambda x\right)^2} \tag{5}$$

where Δx represents the first-order difference of the residual sequence; λ represents the slope obtained from a linear fit to Δx and Δt.

The specific derivation steps of the formula can be obtained from (Smith and Boers 2023b). From the properties of the logarithmic function in Equations (3) and (4), it can be observed that this corresponds to r_* being a smaller negative number, that is, the smaller r_*, the higher the resilience.

2.2.3 | Evaluating Reliability of Resilience

We defined four reliability indicators to evaluate the ability to assess resilience for each vegetation metric. Specifically, we first defined the ratio of r_{ac1} and r_v as the RAV (r_{ac1}/r_v). Then, areas where the difference between r_{ac1} and r_v was within a factor of four ($0.25 < \text{RAV} < 4$) were selected as high-quality areas given the harsh environment of the TP (Smith and Boers 2023b). Regarding accuracy, the average RAV of the TP ($\overline{\text{RAV}}$) and that of the high-quality areas ($\overline{\text{RAV}_\text{H}}$) were calculated as two indicators. Theoretically, the closer these two indicators are to 1, the more accurate the estimate of resilience (Smith and Boers 2023b).

It may not be sufficient to calculate only these accuracy indicators for evaluating reliability of resilience. Because several factors may lead to a large number of potentially excluded pixels, which reduce the statistical sample of accuracy indicators ($\overline{\text{RAV}}$ and $\overline{\text{RAV}_\text{H}}$) and may introduce errors. For example, image quality may interfere with the time series of vegetation metrics (e.g., cloud pollution, etc.). In addition, it may not be possible to solve for the r_{ac1} and r_v of all pixels due to the presence of logarithms in Equations (3) and (4). We thus further evaluated coverage indicators to address these issues. It also includes two metrics, which are the ratio of the area with solvable resilience to the total area (solvable pixel ratio, SPR) and the ratio of the high-quality area to the total area (high-quality pixel ratio, HPR). These two indicators can represent the sample size, and the closer they are to 100% the better the ability to estimate resilience.

2.2.4 | Estimating Trends in Resilience

We implemented overlapping sliding windows to assess the resilience changes in the long-term time series, in which a window size of 60 months is set as in previous studies (Verbesselt et al. 2016; Wang et al. 2023). For each vegetation metric residual across all pixels, we calculated the r_{ac1} and r_v for each window to derive resilience series. The Mann–Kendall test (Hamed and Ramachandra Rao 1998) was employed to evaluate the trends of resilience. A trend with a p value less than 0.05 was deemed a significant change. For each pixel, resilience was deemed to exhibit a high-confidence trend when both indicators (r_{ac1} and r_v) significantly changed in the same direction. If one indicator showed significant change while the other did not exhibit significant change in the opposite direction, we inferred a potential trend in resilience. Conversely, if neither indicator displayed significant changes or if they changed in opposite directions, no apparent trend was discerned.

3 | Results

3.1 | Reliable Vegetation Metrics for Estimating Resilience

We used the monthly mean synthetic scheme in assessing the reliability of each vegetation metric to estimate resilience. The maximum and median synthetic schemes were also compared, but they had lower values for all four reliability indicators (Table S3). Insights drawn from mean synthesis highlight variations in the accuracy of different vegetation metrics (Figure 2). In overview, NIRv is the best performing metric, followed by GOSIF. NIRv has the second highest $\overline{\text{RAV}}$ (0.316) and $\overline{\text{RAV}_\text{H}}$ (0.360), slightly lower than GOSIF (0.328 and 0.381). However, both NIRv's SPR (89.68%) and HPR (65.85%) are much higher than GOSIF (74.50% and 53.87%). EVI and NDVI also demonstrate credibility, with the accuracy indicators of EVI slightly exceeding that of NDVI, but slightly smaller coverage indicators compared to NDVI. Other vegetation metrics performed less satisfactorily. Although kNDVI, LAI, and RTSIF only marginally reduced their $\overline{\text{RAV}}$ and $\overline{\text{RAV}_\text{H}}$ compared with the aforementioned metrics, the HPR for these was merely half or even lower than that of NIRv. GPP and VOD exhibited even poorer performance in both estimation accuracy and coverage. In brief, NIRv, GOSIF, EVI, and NDVI displayed relatively high reliability, among which NIRv offering more accurate estimates of vegetation resilience for a larger number of pixels. Both the estimation accuracy and coverage contribute to NIRv being a reliable vegetation metric for estimating vegetation resilience on the TP.

3.2 | Patterns of Vegetation Resilience on the TP

We used r_{ac1} calculated by NIRv as a proxy to analyze spatial patterns of resilience on the TP (Figure 3). The depiction of vegetation resilience on the TP presents a mixed picture. Vegetation

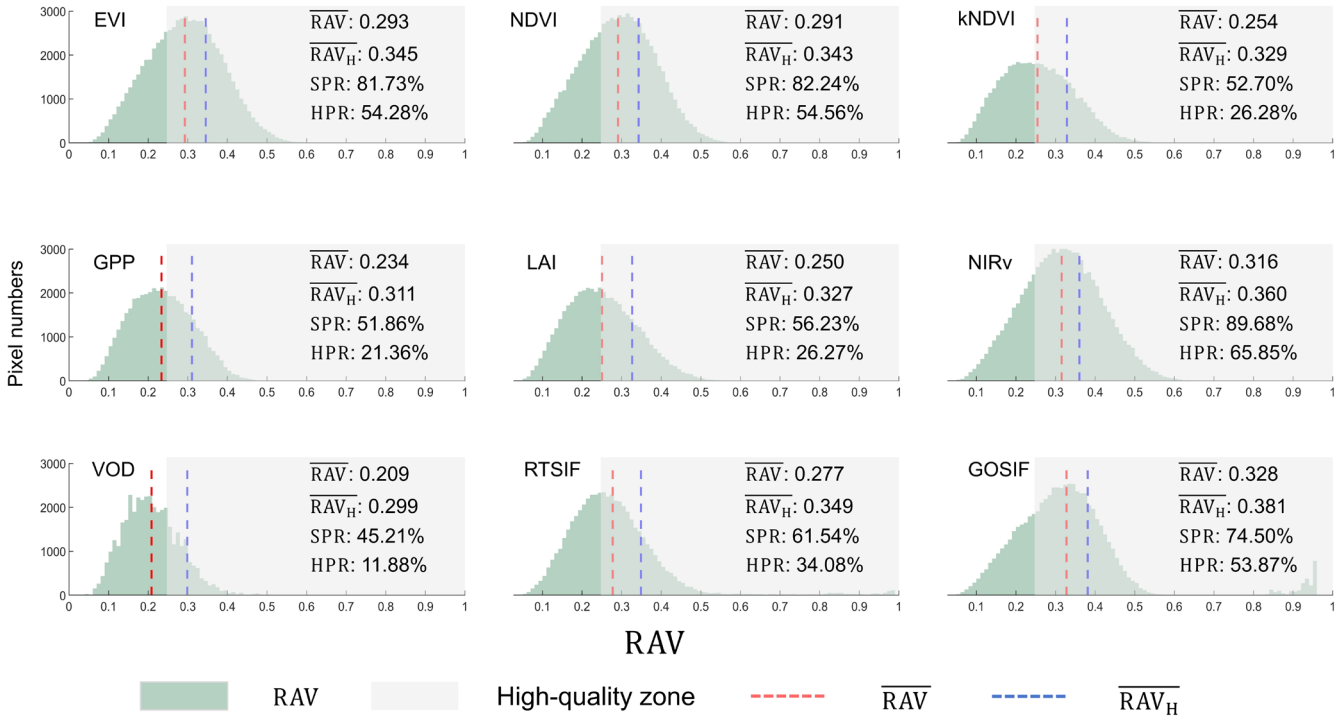

FIGURE 2 | Performance of various vegetation metrics in estimating vegetation resilience. Green regions represent the distribution of the RAV (r_{ac1} / r_v), gray range defines the high-quality zone (differences within a factor of four). Red and blue dashed lines represent the mean RAV of all pixels ($\overline{RAV}$) and high-quality pixels ($\overline{RAV_H}$), respectively. [Colour figure can be viewed at wileyonlinelibrary.com]

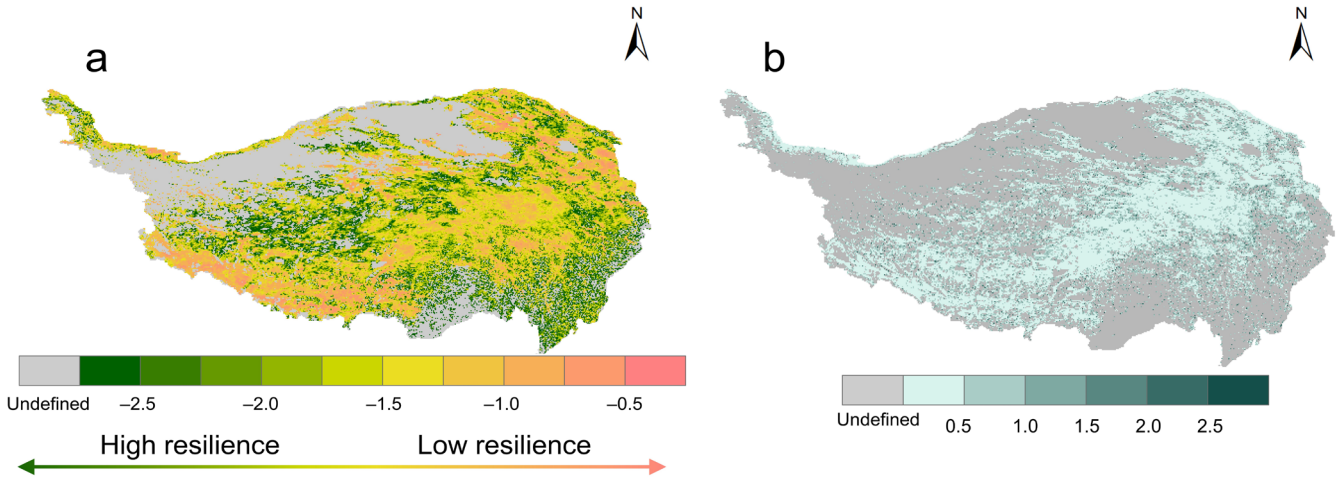

FIGURE 3 | Spatial pattern of vegetation resilience (a) and error (b) on the TP from 2000 to 2022. Smaller r_{ac1} indicates higher resilience. The error is represented by the standard deviation of relatively reliable NIRv, EVI, NDVI, and GOSIF. [Colour figure can be viewed at wileyonlinelibrary.com]

resilience is relatively high in Hengduan Mountains, Qiangtang Plateau, and northeastern Qilian Mountains, while it is lower in Himalayan Mountains, Three Rivers Source Region, and eastern Qilian Mountains. This pattern closely aligns with vegetation distribution (Table S4). Forests, mostly in the southeast, show the highest resilience (r_{ac1} = −2.44), followed by shrubs (r_{ac1} = −1.97). Grasslands in central TP display lower resilience (r_{ac1} = −1.69), but higher than meadows and alpine vegetation (both r_{ac1} = −1.59).

Vegetation resilience also correlates with elevation (Table S4), remaining stable below 5000 m but declining at higher altitudes. Eco-geographical zoning further highlights resilience differences, with the VA zone having the highest resilience. HIC and HID in plateau subcold zone are more resilient than the warmer HIIC and HIID, but less resilient than the wetter HIIAB.

3.3 | Resilience Trends of the TP

Vegetation resilience across 21.48%–30.02% on the TP has undergone substantial changes during the past two decades, with areas of significant loss being 1.16–1.44 times larger than areas of gain (Figure 4a). This trend was sharply captured by NIRv and similarly observed by GOSIF, EVI, and NDVI. However,

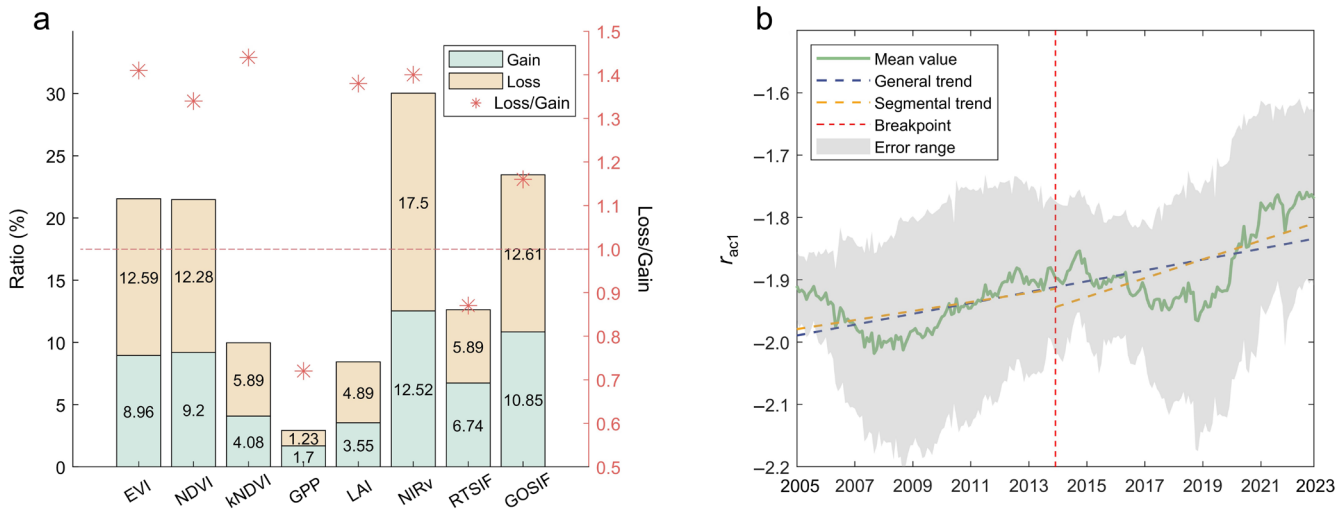

FIGURE 4 | Ratio of resilience gain and loss estimated by different vegetation metrics (a) and resilience trend on the TP from 2000 to 2022 (b). Green curve in (b) represents the NIRv-based resilience, red dashed line is the segmentation line, and yellow dashed line represents the trend of the previous and subsequent segments. The error range is determined by the standard deviation of NIRv, EVI, NDVI, and GOSIF. [Colour figure can be viewed at wileyonlinelibrary.com]

other vegetation metrics underestimated or misinterpreted the resilience trends on the TP.

Pixel-level analysis reveals a significant decline in resilience on the TP over the past two decades, despite fluctuations (Figure 4b). After a brief increase in the early 21st century, the resilience declined, followed by a slight rise after 2014, and then a sharp decline. The extreme points of the fitted curve identify 2014 as a turning point (Figure S2). In the decade following this point, the rate of resilience declines more than doubled compared to the previous period.

We further conducted separate estimations the spatial pattern of resilience trends using r_{ac1} and r_v for the complete time series (Figure 5a) and segmented time series (Figure 5b,c). The picture for long-term resilience trends in TP is mixed. Results indicate that 47.49% of the TP area exhibits at least one indicator signaling a decline in resilience, markedly surpassing the proportion of areas displaying increased resilience (30.64%) over the entire period from 2000 to 2022. Regions experiencing substantial resilience loss are primarily clustered in the Three Rivers Source Region and the western Himalayan Mountains. In addition, signs of resilience decline are also observable in the western Qilian Mountains and Kunlun Mountains. Conversely, areas demonstrating resilience gains are predominantly found around Qinghai Lake and the Zoige grasslands in the eastern part of the TP and can also be observed in the central and southern parts of the TP.

The complexity persists when examining the half of the time series. Although statistically there seems to be little difference between the two periods (before and after 2014): the proportion of resilience loss increased from 40.95% to 44.84%, and resilience gain decreased from 35.53% to 33.70%, the pattern of resilience trends starkly differs. Resilience in the western Qilian Mountains and the Three Rivers Source Region changed from increasing to decreasing, while in the western Kunlun Mountains and the eastern Himalayan Mountains, it changed from decreasing to increasing. Notably, the Qiangtang Plateau, the western Himalayan Mountains, and almost the entire Three Rivers Source Region experienced a loss of resilience in any given time series.

3.4 | Spatial Variability of Resilience Trends

To further clarify vegetation resilience trends over the past decade, we partitioned the TP into subregions based on three criteria: elevation (Figure 6a), vegetation type (Figure 6b), and eco-geographical conditions (Figure 6c). Vegetation resilience below 4000 m elevation has exhibited a notable increasing trend over the past decade, contrasting with areas above 4000 m, which are experiencing significant losses. Although a temporary resilience surge occurred at higher elevations around 2018, it failed to halt the overall decline. Resilience trends vary across vegetation types, with significantly increasing resilience in forest and shrub and consistently decreasing resilience in meadow, steppe, and alpine vegetation. Concerning eco-geographic subregions, vegetation resilience increased in the relatively warm and wet VA and HIIC regions significantly, with no discernible trend in the HIIAB. Conversely, the HID region, typifying cold and arid environments, experienced a sharp decline in vegetation resilience. Noticeable decreased in resilience is also observed in the HIC, HIB, and HIID regions.

4 | Discussion

4.1 | Reliability of Remotely Sensed Resilience

Estimating the spatial pattern and temporal trends of vegetation resilience on the TP has been a long-standing issue. The adoption of critical slowing down theory alongside long-term remote sensing data has emerged as a promising solution, steadily gaining traction. A fundamental question arises regarding the selection of vegetation metrics to enhance the reliability of resilience estimation. Although pioneering experiments were carried out

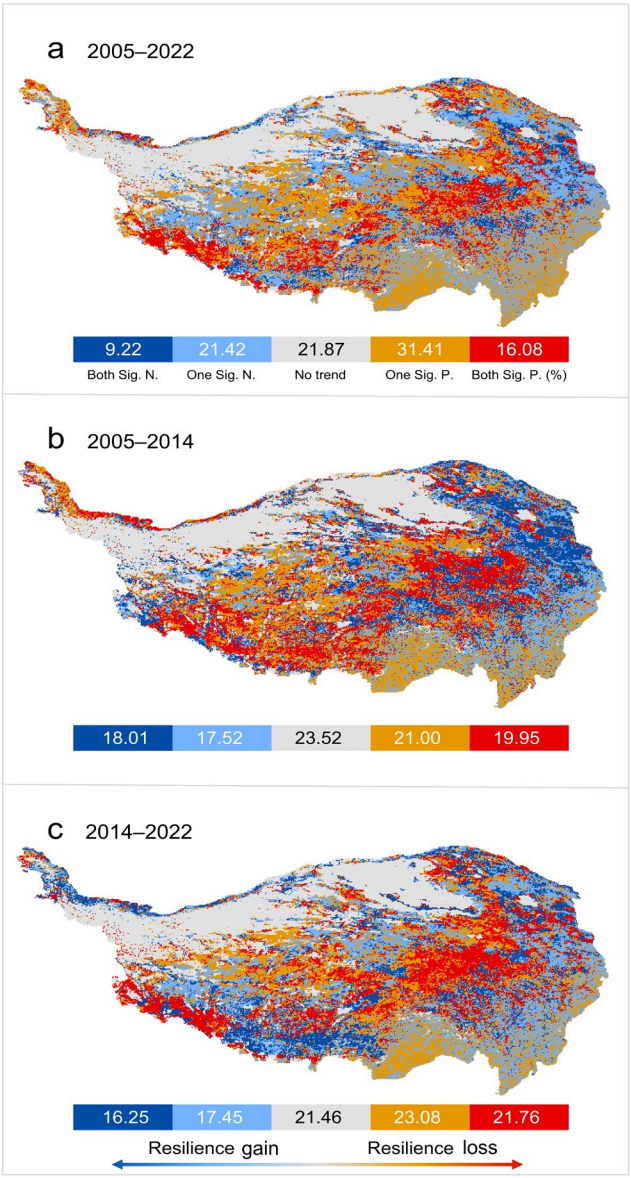

FIGURE 5 | Resilience trends of the whole time series (a), before (b), and after 2014 (c) on the TP. Both (one) Sig. N. (P.) means both r_{ac1} and r_v (one of them) decreased (increased) at the level of $p < 0.05$. Gray areas denote either no vegetation covers or the absence of a consistent trend, red and orange areas indicate resilience loss, while dark blue and light blue areas indicate resilience gain. [Colour figure can be viewed at wileyonlinelibrary.com]

globally (Smith and Boers 2023b), distinct conclusions may arise for specific regions, as evidenced by our study.

We defined four metrics describing the ability of vegetation indices to estimate resilience in terms of both accuracy and coverage. RAV is a generalized indicator for assessing the accuracy of resilience estimates, and we thus calculated average value for each vegetation metrics on the entire TP ($\overline{\text{RAV}}$), which represent the overall accuracy. Additionally the RAV of high-quality pixels ($\overline{\text{RAV}_{\text{H}}}$) was also evaluated, which could avoid extreme values. These two indicators are robust for a constant number of samples, but may lead to errors if the number of samples changes with the vegetation index. We therefore additionally calculated the ratio of all (SPR) and high-quality pixels (HPR) with solvable resilience in order to assess the sample size for statistical significance. These indicators can inform future assessments of the reliability of resilience estimates, especially for large-scale studies.

Our experiment results suggest that mean synthesis may offer a more suitable approach on the TP (Table S3). As the MODIS service time extends, employing mean synthesis may mitigate systematic errors stemming from sensor aging. This study underscores the suitability of remote-sensing datasets for resilience analyzes on the TP. The effectiveness of vegetation metrics to estimate resilience varies across different ecosystems and regions. Acceptance of recommendations directly from global scales (Guo, Zhu, and Gong 2024; Smith and Boers 2023b) or other regions (Boulton, Lenton, and Boers 2022; Wang et al. 2023) may result in the underestimation or misestimation of resilience trends on the TP.

We recommend utilizing NIRv as a more reliable estimator for resilience on the TP, followed by GOSIF, EVI, and NDVI. The VOD we tested is a typical example where the additional error introduced by varying signal-to-noise ratios in cross-sensor data resulted in poor estimation outcomes (Smith et al. 2023). Such datasets can be excluded a priori. In addition, the use of VOD may not be theoretically feasible for the TP. Due to the high penetration capacity of passive microwaves, VOD may be subject to severe soil water disturbance compared with changes in vegetation leaf water content on the low biomass TP. Previous study indicated that the saturation effect of NDVI makes it unsuitable for estimating vegetation resilience in high biomass regions (Smith and Boers 2023b), but our study provides no evidence. Our results show that NDVI is more reliable compared to most other metrics (Figure 2) and improvements such as the EVI and kNDVI did not improve reliability. This may be related to the vegetation types and growth conditions in the study area. The main vegetation types on the TP are alpine meadows and grasslands, where low biomass and poor growing conditions likely reduce the influence of the saturation effect as a limiting factor. We hypothesize that soil and snow disturbances may limit the accuracy of these metrics, as they interfere with vegetation signals and introduce errors (Smith and Boers 2023b; Wang et al. 2013). The strong performance of NIRv and SIF is not unexpected. Relative to other vegetation metrics, they possess a more explicit physical meaning, describing the ability of vegetation canopies to capture and utilize light energy, and exhibiting lower sensitivity to soil background (Badgley et al. 2019; Badgley, Field, and Berry 2017). We hypothesize that estimates of vegetation resilience may depend primarily on the chlorophyll content of the vegetation rather than the number of leaves. For example, in arid regions, vegetation may choose the strategy of reducing leaf area and number to maintain leaf water content, but they may have higher resilience (Chen et al. 2020; Li et al. 2018). This may be the reason why metrics related to chlorophyll content like NIRv and SIF are more reliable.

4.2 | Causes of Resilience Variation on the TP

Our quantification of resilience patterns and trends on the TP contributes to a deeper understanding of the plateau's vulnerability. We found that vegetation resilience is low in the Western

FIGURE 6 | Spatial heterogeneity of vegetation resilience is manifested in elevation (a), vegetation types (b), and ecological-geographical zones (c), with the time series segmented by the gray areas around 2014. The ↑ (↓) in the legend represents a significant increase (decrease) in the corresponding curve after 2014, which represents a significant loss (gain) in resilience. [Colour figure can be viewed at wileyonlinelibrary.com]

Himalayas, the southeastern Qilian Mountains, and the Three Rivers Source Region. This aligns with previous conclusions (Li, Zhang, et al. 2020; Yang et al. 2022), but we demonstrate more pronounced internal variations. The resilience pattern shows a clear altitudinal differentiation: as elevation increases, resilience decreases (Table S4). This may be related to the harsh conditions in high-altitude areas, such as cold spells (Lu et al. 2023), severe wind erosion, and strong radiation (Piao et al. 2019), which may damage the root systems of vegetation. Additionally, studies have shown that the similarity between seed banks and aboveground vegetation decreases with increasing elevation, which explains the reduction in resilience (An, Zhao, and Ma 2020; Ma et al. 2019).

Usually forests and shrubs are highly stable rather than resilient (Yao et al. 2022; Yao, Liu, Song, et al. 2024), but we found that forests and shrubs on the TP are highly resilient (Table S4). We consider that this may be related to the type and intensity of the disturbance. It may indeed take longer for forests to reestablish due to the hysteresis of catastrophic disturbances (Scheffer et al. 2001). However, methods based on critical slowing down can measure the relation between minor disturbances and resilience, and are not limited to a particular disturbance type. In this case, forests can still recover quickly. We also suggest that steppes are more resilient than meadows. Steppes have higher chlorophyll content, smaller leaf area, and more dry matter than meadows, thus have higher water use efficiency and contribute to rapid recovery from disturbances (Li et al. 2018). Meadows that grow in warmer and wetter conditions are more sensitive to drought and less likely to recover (Li, Wu, et al. 2020). In addition, widely distributed steppes occupy more ecological niches on the TP, resulting in a greater adaptation to variable climates (Li, Wu, et al. 2020).

Hydrothermal conditions provide another explanation for the resilience patterns on the TP. We found that although both HIC and HIB are in the Plateau subcold zone, the more arid HIC is more resilient. This is because vegetation in arid environments has evolved to be more adapted to drought and has weaker drought legacy effects (Li, Zhu, et al. 2020). Once sufficient moisture and sunlight were available after a disturbance, low-lying

vegetation can recover rapidly, even surpassing pre-disturbance levels (Chen et al. 2020). We also observed that when water is a limiting factor, cold regions like HIC have higher resilience than the warmer HIIC. Increasing temperatures may increase water evaporation and reduce water availability, resulting in resilience loss (Piao et al. 2019). In addition, high temperatures are not always favorable for nonforest vegetation on the TP. When temperatures exceed the optimal level of 14.7°C, active enzymes may degrade, and stomata may close, hindering vegetation recovery (Chen et al. 2021; Zhang et al. 2023).

4.3 | Driven Factors of Resilience on the TP

We found a severe loss of resilience in the Himalayas and the Three Rivers Source Region, a slight loss of resilience in the southern forests, and an increase trend in the Zoige grasslands over the past 20 years. Moisture is often considered to be the main influence on resilience changes (Smith and Boers 2023a). Water scarcity not only diminishes ecosystem resilience but can also lead to unforeseen ecosystem shifts (Flores et al. 2024). While adequate winter precipitation replenishes groundwater and increases water availability for subdominant species (Ladwig et al. 2016). Recent findings indicating a severe decline in terrestrial water storage on the TP over the past two decades, particularly in the southern TP and the Three Rivers Source Region (Li et al. 2022), which may lead to the continued loss of resilience in both regions.

Soil erosion is another factor that reduces resilience, as vegetation resilience and soil are coupled within a system (Gao et al. 2019). Soil erodibility has decreased significantly in the southern part of the TP over the last 40 years (Lin et al. 2023). This may be detrimental to plant storage of carbon and nitrogen in subsurface crowns and roots, and may also reduce the soil seed bank (Ma et al. 2019), triggering a decline in resilience in the Himalayas. Inappropriate land development, excessive deforestation, and overgrazing also have negative effects on ecosystems (Liu et al. 2018, 2024), leading to accelerated loss of resilience. For example, a significant increase in grazing intensity has been documented in the Three Rivers Source Region and Qilian Mountain since 2000 (Li et al. 2021; Zhu et al. 2023), which is reflected in the decline in resilience. Although the Zoige grassland is also an important pastureland, both our study and previous works suggest that resilience in this region is increasing (Ji et al. 2024). This may because human activities have not always been intense here (Li et al. 2021), and ecological restoration efforts have been implemented (Ji et al. 2024). This may put it in a position of intermediate disturbance that favors high resilience (Grime 1973; Li, Zhang, et al. 2020).

The impact of natural disasters on resilience cannot be ignored. Extreme wet or dry conditions (Hubbart, Guyette, and Muzika 2016; Smith and Boers 2023a), reduced snowpack (Rixen et al. 2012), insect infestations (Castagneri et al. 2020), and earthquakes (Gao et al. 2024; Pandey et al. 2023) can all severely damage resilience. For example, insect outbreaks can reduce tree biomass accumulation and affect xylem formation in woody plants (Castagneri et al. 2020). Reduced winter snowpack can expose vegetation root systems to harsh conditions (Liu et al. 2022; Wang et al. 2018). Additionally, tree recovery time has been shown to have a negative correlation with the distance from earthquake epicenters (Pandey et al. 2023), suggesting that the frequent crustal movements on the TP may be a contributing factor to the decline in vegetation resilience.

4.4 | Limitations and Perspectives

While we experimented with nine commonly used vegetation metrics to estimate resilience in this study, it would be premature to say that we have arrived at definitive conclusions on the TP. Even the best-performing metric still fall short of ideal results. There is still much work to be done in both refining vegetation metrics and enhancing methods of time series decomposition. Additionally, the connotation of vegetation resilience and the drivers of change have been puzzling, requiring further quantification in the future. Finally, changes in resilience are frequently associated with climate change, while we aim to strengthen the connection between resilience and ecological restoration projects in the future to assess whether they are effectively bolstering vegetation resilience as intended.

5 | Conclusion

In this study, we demonstrate the vulnerability of the TP from the perspective of reduced resilience. Our findings indicate that monthly mean synthesized NIRv could better construct residual time series for assessing resilience on the TP. We observed low resilience on the northeastern and southwestern edges of the TP and in the Three River Source region. Over the past two decades, resilience on the TP exhibited an accelerated decline, with the area of resilience loss being approximately 1.16–1.44 times that of the increase. The results provide a solid foundation and preliminary understanding for future study. We suggest that resilience should be more considered in the evaluation criteria of ecosystem functions and services, which will well complement the inadequacy of remote sensing-based vegetation greenness perception of ecosystems. Moreover, more attention and protection of the TP are warranted, particularly in regions experiencing declining resilience.

Acknowledgments

This study was supported by National Natural Science Foundation of China (Grant No. 42171307) and the "GeoX" Interdisciplinary Research Funds for the Frontiers Science Center for Critical Earth Material Cycling, Nanjing University. The authors are grateful to the High-Performance Computing Center, Nanjing University, for computational support.

Data Availability Statement

The data that support the findings of this study are available from the corresponding author upon reasonable request.

References

An, H., Y. Zhao, and M. Ma. 2020. "Precipitation Controls Seed Bank Size and Its Role in Alpine Meadow Community Regeneration With Increasing Altitude." *Global Change Biology* 26, no. 10: 5767–5777. https://doi.org/10.1111/gcb.15260.

An, R., C. Zhang, M. Sun, et al. 2021. "Monitoring Grassland Degradation and Restoration Using a Novel Climate Use Efficiency (NCUE) Index in the Tibetan Plateau, China." *Ecological Indicators* 131: 108208. https://doi.org/10.1016/j.ecolind.2021.108208.

Badgley, G., L. D. L. Anderegg, J. A. Berry, and C. B. Field. 2019. "Terrestrial Gross Primary Production: Using NIR_V to Scale From Site to Globe." *Global Change Biology* 25, no. 11: 3731–3740. https://doi.org/10.1111/gcb.14729.

Badgley, G., C. B. Field, and J. A. Berry. 2017. "Canopy Near-Infrared Reflectance and Terrestrial Photosynthesis." *Science Advances* 3, no. 3: e1602244. https://doi.org/10.1126/sciadv.1602244.

Bathiany, S., R. Bastiaansen, A. Bastos, et al. 2024. "Ecosystem Resilience Monitoring and Early Warning Using Earth Observation Data: Challenges and Outlook." *Surveys in Geophysics*. https://doi.org/10.1007/s10712-024-09833-z.

Boulton, C. A., T. M. Lenton, and N. Boers. 2022. "Pronounced Loss of Amazon Rainforest Resilience Since the Early 2000s." *Nature Climate Change* 12, no. 3: 271–278. https://doi.org/10.1038/s41558-022-01287-8.

Camps-Valls, G., M. Campos-Taberner, Á. Moreno-Martínez, et al. 2021. "A Unified Vegetation Index for Quantifying the Terrestrial Biosphere." *Science Advances* 7, no. 9: eabc7447. https://doi.org/10.1126/sciadv.abc7447.

Castagneri, D., A. L. Prendin, R. L. Peters, M. Carrer, G. von Arx, and P. Fonti. 2020. "Long-Term Impacts of Defoliator Outbreaks on Larch Xylem Structure and Tree-Ring Biomass." *Frontiers in Plant Science* 11: 1078. https://doi.org/10.3389/fpls.2020.01078.

Chen, A., L. Huang, Q. Liu, and S. Piao. 2021. "Optimal Temperature of Vegetation Productivity and Its Linkage With Climate and Elevation on the Tibetan Plateau." *Global Change Biology* 27, no. 9: 1942–1951. https://doi.org/10.1111/gcb.15542.

Chen, F., W. Man, S. Wang, et al. 2023. "Southeast Asian Ecological Dependency on Tibetan Plateau Streamflow Over the Last Millennium." *Nature Geoscience* 16, no. 12: 1151–1158. https://doi.org/10.1038/s41561-023-01320-1.

Chen, H., Q. Zhu, C. Peng, et al. 2013. "The Impacts of Climate Change and Human Activities on Biogeochemical Cycles on the Qinghai-Tibetan Plateau." *Global Change Biology* 19, no. 10: 2940–2955. https://doi.org/10.1111/gcb.12277.

Chen, N., Y. Zhang, J. Zu, et al. 2020. "The Compensation Effects of Post-Drought Regrowth on Earlier Drought Loss Across the Tibetan Plateau Grasslands." *Agricultural and Forest Meteorology* 281: 107822. https://doi.org/10.1016/j.agrformet.2019.107822.

Chen, X., Y. Huang, C. Nie, et al. 2022. "A Long-Term Reconstructed TROPOMI Solar-Induced Fluorescence Dataset Using Machine Learning Algorithms." *Scientific Data* 9, no. 1: 427. https://doi.org/10.1038/s41597-022-01520-1.

Dakos, V., S. R. Carpenter, W. A. Brock, et al. 2012. "Methods for Detecting Early Warnings of Critical Transitions in Time Series Illustrated Using Simulated Ecological Data." *PLoS One* 7, no. 7: e41010. https://doi.org/10.1371/journal.pone.0041010.

Dakos, V., and S. Kéfi. 2022. "Ecological Resilience: What to Measure and How." *Environmental Research Letters* 17, no. 4: 043003. https://doi.org/10.1088/1748-9326/ac5767.

De Keersmaecker, W., S. Lhermitte, L. Tits, O. Honnay, B. Somers, and P. Coppin. 2015. "A Model Quantifying Global Vegetation Resistance and Resilience to Short-Term Climate Anomalies and Their Relationship With Vegetation Cover." *Global Ecology and Biogeography* 24, no. 5: 539–548. https://doi.org/10.1111/geb.12279.

Fang, O., and Q.-B. Zhang. 2019. "Tree Resilience to Drought Increases in the Tibetan Plateau." *Global Change Biology* 25, no. 1: 245–253. https://doi.org/10.1111/gcb.14470.

Flores, B. M., E. Montoya, B. Sakschewski, et al. 2024. "Critical Transitions in the Amazon Forest System." *Nature* 626, no. 7999: 555–564. https://doi.org/10.1038/s41586-023-06970-0.

Forzieri, G., V. Dakos, N. G. McDowell, A. Ramdane, and A. Cescatti. 2022. "Emerging Signals of Declining Forest Resilience Under Climate Change." *Nature* 608, no. 7923: 534–539. https://doi.org/10.1038/s41586-022-04959-9.

Fu, T., E. Liang, X. Lu, et al. 2020. "Tree Growth Responses and Resilience After the 1950-Zayu-Medog Earthquake, Southeast Tibetan Plateau." *Dendrochronologia* 62: 125724. https://doi.org/10.1016/j.dendro.2020.125724.

Gao, S., E. Liang, R. Liu, et al. 2024. "Shifts of Forest Resilience After Seismic Disturbances in Tectonically Active Regions." *Nature Geoscience* 17, no. 3: 189–196. https://doi.org/10.1038/s41561-024-01380-x.

Gao, X., S. Dong, Y. Xu, et al. 2019. "Resilience of Revegetated Grassland for Restoring Severely Degraded Alpine Meadows Is Driven by Plant and Soil Quality Along Recovery Time: A Case Study From the Three-River Headwater Area of Qinghai-Tibetan Plateau." *Agriculture, Ecosystems & Environment* 279: 169–177. https://doi.org/10.1016/j.agee.2019.01.010.

Gorelick, N., M. Hancher, M. Dixon, S. Ilyushchenko, D. Thau, and R. Moore. 2017. "Google Earth Engine: Planetary-Scale Geospatial Analysis for Everyone." *Remote Sensing of Environment* 202: 18–27. https://doi.org/10.1016/j.rse.2017.06.031.

Grime, J. P. 1973. "Competitive Exclusion in Herbaceous Vegetation." *Nature* 242, no. 5396: 344–347. https://doi.org/10.1038/242344a0.

Guo, J., Z. Zhu, and P. Gong. 2024. "Global Forest Resilience Change From 2001 to 2022." *International Journal of Remote Sensing* 45, no. 17: 5889–5900. https://doi.org/10.1080/01431161.2024.2380546.

Hamed, K. H., and A. Ramachandra Rao. 1998. "A Modified Mann-Kendall Trend Test for Autocorrelated Data." *Journal of Hydrology* 204, no. 1: 182–196. https://doi.org/10.1016/S0022-1694(97)00125-X.

Hu, Y., F. Wei, B. Fu, S. Wang, W. Zhang, and Y. Zhang. 2023. "Changes and Influencing Factors of Ecosystem Resilience in China." *Environmental Research Letters* 18, no. 9: 94012. https://doi.org/10.1088/1748-9326/acec89.

Hubbart, J. A., R. Guyette, and R.-M. Muzika. 2016. "More Than Drought: Precipitation Variance, Excessive Wetness, Pathogens and the Future of the Western Edge of the Eastern Deciduous Forest." *Science of the Total Environment* 566–567: 463–467. https://doi.org/10.1016/j.scitotenv.2016.05.108.

Ji, Z., S. Zou, W. Zhang, F. Song, T. Yuan, and B. Xu. 2024. "Optimizing Zoning for Ecological Management in Alpine Region by Combining Ecosystem Service Supply and Demand With Ecosystem Resilience." *Journal of Environmental Management* 365: 121508. https://doi.org/10.1016/j.jenvman.2024.121508.

Ladwig, L. M., Z. R. Ratajczak, T. W. Ocheltree, et al. 2016. "Beyond Arctic and Alpine: The Influence of Winter Climate on Temperate Ecosystems." *Ecology* 97, no. 2: 372–382. https://doi.org/10.1890/15-0153.1.

Li, C., H. Wulf, B. Schmid, J. S. He, and M. E. Schaepman. 2018. "Estimating Plant Traits of Alpine Grasslands on the Qinghai-Tibetan Plateau Using Remote Sensing." *IEEE Journal of Selected Topics in Applied Earth Observations and Remote Sensing* 11, no. 7: 2263–2275. https://doi.org/10.1109/JSTARS.2018.2824901.

Li, M., J. Wu, Y. He, et al. 2020. "Dimensionality of Grassland Stability Shifts Along With Altitudes on the Tibetan Plateau." *Agricultural and Forest Meteorology* 291: 108080. https://doi.org/10.1016/j.agrformet.2020.108080.

Li, M., X. Zhang, Y. He, B. Niu, and J. Wu. 2020. "Assessment of the Vulnerability of Alpine Grasslands on the Qinghai-Tibetan Plateau." *PeerJ* 8: e8513. https://doi.org/10.7717/peerj.8513.

Li, M., X. Zhang, J. Wu, Q. Ding, B. Niu, and Y. He. 2021. "Declining Human Activity Intensity on Alpine Grasslands of the Tibetan Plateau." *Journal of Environmental Management* 296: 113198. https://doi.org/10.1016/j.jenvman.2021.113198.

Li, P., D. Zhu, Y. Wang, and D. Liu. 2020. "Elevation Dependence of Drought Legacy Effects on Vegetation Greenness Over the Tibetan Plateau." *Agricultural and Forest Meteorology* 295: 108190. https://doi.org/10.1016/j.agrformet.2020.108190.

Li, X., D. Long, B. R. Scanlon, et al. 2022. "Climate Change Threatens Terrestrial Water Storage Over the Tibetan Plateau." *Nature Climate Change* 12, no. 9: 801–807. https://doi.org/10.1038/s41558-022-01443-0.

Li, X., and J. Xiao. 2019. "A Global, 0.05-Degree Product of Solar-Induced Chlorophyll Fluorescence Derived From OCO-2, MODIS, and Reanalysis Data." *Remote Sensing* 11, no. 5: 517.

Li, Y., R. Xu, K. Yang, et al. 2023. "Contribution of Tibetan Plateau Ecosystems to Local and Remote Precipitation Through Moisture Recycling." *Global Change Biology* 29, no. 3: 702–718. https://doi.org/10.1111/gcb.16495.

Lin, H., X. Cheng, L. A. Bruijnzeel, et al. 2023. "Land Degradation and Climate Change Lessened Soil Erodibility Across a Wide Area of the Southern Tibetan Plateau Over the Past 35–40 Years." *Land Degradation & Development* 34, no. 9: 2636–2651. https://doi.org/10.1002/ldr.4636.

Liu, H., P. Xiao, X. Zhang, and Y. Wu. 2023. "Increased Snow Cover Enhances Gross Primary Productivity in Cold and Dry Regions of the Tibetan Plateau." *Ecosphere* 14, no. 9: e4656. https://doi.org/10.1002/ecs2.4656.

Liu, S., K. Zamanian, P.-M. Schleuss, M. Zarebanadkouki, and Y. Kuzyakov. 2018. "Degradation of Tibetan Grasslands: Consequences for Carbon and Nutrient Cycles." *Agriculture, Ecosystems & Environment* 252: 93–104. https://doi.org/10.1016/j.agee.2017.10.011.

Liu, X., W. Zhao, Y. Yao, and P. Pereira. 2024. "The Rising Human Footprint in the Tibetan Plateau Threatens the Effectiveness of Ecological Restoration on Vegetation Growth." *Journal of Environmental Management* 351: 119963. https://doi.org/10.1016/j.jenvman.2023.119963.

Liu, Y., W. Zhou, S. Gao, X. Ma, and K. Yan. 2022. "Phenological Responses to Snow Seasonality in the Qilian Mountains Is a Function of Both Elevation and Vegetation Types." *Remote Sensing* 14, no. 15: 3629.

Lu, X., F. Hu, E. Liang, S. R. Sigdel, Z. Shang, and J. J. Camarero. 2023. "Loss of Growth Resilience Towards the Alpine Shrubline." *Forest Ecology and Management* 539: 121013. https://doi.org/10.1016/j.foreco.2023.121013.

Ma, M., C. C. Baskin, W. Li, et al. 2019. "Seed Banks Trigger Ecological Resilience in Subalpine Meadows Abandoned After Arable Farming on the Tibetan Plateau." *Ecological Applications* 29, no. 7: e01959. https://doi.org/10.1002/eap.1959.

Pan, N., X. Feng, B. Fu, S. Wang, F. Ji, and S. Pan. 2018. "Increasing Global Vegetation Browning Hidden in Overall Vegetation Greening: Insights From Time-Varying Trends." *Remote Sensing of Environment* 214: 59–72. https://doi.org/10.1016/j.rse.2018.05.018.

Pandey, J., J. J. Camarero, X. Lu, S. R. Sigdel, S. Gao, and E. Liang. 2023. "Forest Resilience in the Himalayas Inferred From Tree Growth After Earthquake Disturbances." *Journal of Geophysical Research: Biogeosciences* 128, no. 9: e2023JG007502. https://doi.org/10.1029/2023JG007502.

Piao, S. L., X. Z. Zhang, T. Wang, et al. 2019. "Responses and Feedback of the Tibetan Plateau's Alpine Ecosystem to Climate Change." *Chinese Science Bulletin-Chinese* 64, no. 27: 2842–2855. https://doi.org/10.1360/tb-2019-0074.

Rixen, C., M. A. Dawes, S. Wipf, and F. Hagedorn. 2012. "Evidence of Enhanced Freezing Damage in Treeline Plants During Six Years of CO_2 Enrichment and Soil Warming." *Oikos* 121, no. 10: 1532–1543. https://doi.org/10.1111/j.1600-0706.2011.20031.x.

Sawada, Y., H. Tsutsui, T. Koike, M. Rasmy, R. Seto, and H. Fujii. 2016. "A Field Verification of an Algorithm for Retrieving Vegetation Water Content From Passive Microwave Observations." *IEEE Transactions on Geoscience and Remote Sensing* 54, no. 4: 2082–2095. https://doi.org/10.1109/TGRS.2015.2495365.

Scheffer, M., J. Bascompte, W. A. Brock, et al. 2009. "Early-Warning Signals for Critical Transitions." *Nature* 461, no. 7260: 53–59. https://doi.org/10.1038/nature08227.

Scheffer, M., S. Carpenter, J. A. Foley, C. Folke, and B. Walker. 2001. "Catastrophic Shifts in Ecosystems." *Nature* 413, no. 6856: 591–596. https://doi.org/10.1038/35098000.

Smith, T., and N. Boers. 2023a. "Global Vegetation Resilience Linked to Water Availability and Variability." *Nature Communications* 14, no. 1: 498. https://doi.org/10.1038/s41467-023-36207-7.

Smith, T., and N. Boers. 2023b. "Reliability of Vegetation Resilience Estimates Depends on Biomass Density." *Nature Ecology & Evolution* 7, no. 11: 1799–1808. https://doi.org/10.1038/s41559-023-02194-7.

Smith, T., D. Traxl, and N. Boers. 2022. "Empirical Evidence for Recent Global Shifts in Vegetation Resilience." *Nature Climate Change* 12, no. 5: 477–484. https://doi.org/10.1038/s41558-022-01352-2.

Smith, T., R. M. Zotta, C. A. Boulton, T. M. Lenton, W. Dorigo, and N. Boers. 2023. "Reliability of Resilience Estimation Based on Multi-Instrument Time Series." *Earth System Dynamics* 14, no. 1: 173–183. https://doi.org/10.5194/esd-14-173-2023.

Teng, Y., J. Zhan, F. B. Agyemang, and Y. Sun. 2020. "The Effects of Degradation on Alpine Grassland Resilience: A Study Based on Meta-Analysis Data." *Global Ecology and Conservation* 24: e01336. https://doi.org/10.1016/j.gecco.2020.e01336.

Verbesselt, J., N. Umlauf, M. Hirota, et al. 2016. "Remotely Sensed Resilience of Tropical Forests." *Nature Climate Change* 6, no. 11: 1028–1031. https://doi.org/10.1038/nclimate3108.

Wang, T., S. Peng, X. Lin, and J. Chang. 2013. "Declining Snow Cover May Affect Spring Phenological Trend on the Tibetan Plateau." *Proceedings of the National Academy of Sciences* 110, no. 31: E2854–E2855. https://doi.org/10.1073/pnas.1306157110.

Wang, X., C. Wu, D. Peng, A. Gonsamo, and Z. Liu. 2018. "Snow Cover Phenology Affects Alpine Vegetation Growth Dynamics on the Tibetan Plateau: Satellite Observed Evidence, Impacts of Different Biomes, and Climate Drivers." *Agricultural and Forest Meteorology* 256–257: 61–74. https://doi.org/10.1016/j.agrformet.2018.03.004.

Wang, Z., B. Fu, X. Wu, et al. 2023. "Vegetation Resilience Does Not Increase Consistently With Greening in China's Loess Plateau." *Communications Earth & Environment* 4, no. 1: 336. https://doi.org/10.1038/s43247-023-01000-3.

Wei, D., Y. Qi, Y. Ma, et al. 2021. "Plant Uptake of CO_2 Outpaces Losses From Permafrost and Plant Respiration on the Tibetan Plateau." *Proceedings of the National Academy of Sciences* 118, no. 33: e2015283118. https://doi.org/10.1073/pnas.2015283118.

Willis, K. J., E. S. Jeffers, and C. Tovar. 2018. "What Makes a Terrestrial Ecosystem Resilient?" *Science* 359, no. 6379: 988–989. https://doi.org/10.1126/science.aar5439.

Wu, S., Q. Yang, and D. Zheng. 2003. "Delineation of Eco-Geographic Regional System of China." *Journal of Geographical Sciences* 13, no. 3: 309–315. https://doi.org/10.1007/BF02837505.

Xia, M., K. Jia, W. Zhao, S. Liu, X. Wei, and B. Wang. 2021. "Spatio-Temporal Changes of Ecological Vulnerability Across the Qinghai-Tibetan Plateau." *Ecological Indicators* 123: 107274. https://doi.org/10.1016/j.ecolind.2020.107274.

Xu, J., and R. E. Grumbine. 2014. "Building Ecosystem Resilience for Climate Change Adaptation in the Asian Highlands." *WIREs Climate Change* 5, no. 6: 709–718. https://doi.org/10.1002/wcc.302.

Yang, Y., Y. Sun, B. Niu, Y. Feng, F. Han, and M. Li. 2022. "Increasing Connections Among Temporal Invariability, Resistance and Resilience of Alpine Grasslands on the Tibetan Plateau." *Frontiers in Plant Science* 13: 1026731. https://doi.org/10.3389/fpls.2022.1026731.

Yao, T., Y. Xue, D. Chen, et al. 2019. "Recent Third Pole's Rapid Warming Accompanies Cryospheric Melt and Water Cycle Intensification and Interactions Between Monsoon and Environment: Multidisciplinary Approach With Observations, Modeling, and Analysis." *Bulletin of the American Meteorological Society* 100, no. 3: 423–444. https://doi.org/10.1175/BAMS-D-17-0057.1.

Yao, Y., B. Fu, Y. Liu, et al. 2022. "Evaluation of Ecosystem Resilience to Drought Based on Drought Intensity and Recovery Time." *Agricultural and Forest Meteorology* 314: 108809. https://doi.org/10.1016/j.agrformet.2022.108809.

Yao, Y., Y. Liu, F. Fu, et al. 2024. "Declined Terrestrial Ecosystem Resilience." *Global Change Biology* 30, no. 4: e17291. https://doi.org/10.1111/gcb.17291.

Yao, Y., Y. Liu, J. Song, et al. 2024. "Declining Tradeoff Between Resistance and Resilience of Ecosystems to Drought." *Earth's Future* 12, no. 5: e2024EF004665. https://doi.org/10.1029/2024EF004665.

Yin, D., X. Gou, H. Yang, K. Wang, and D. Zhang. 2024. "Species-Specific, Size-Dependent, and Environmentally Modulated Growth Resilience to Drought in Conifer Forests on the Eastern Tibetan Plateau." *European Journal of Forest Research* 143, no. 1: 33–43. https://doi.org/10.1007/s10342-023-01604-6.

Zhang, G., Y. Zhang, J. Dong, and X. Xiao. 2013. "Green-Up Dates in the Tibetan Plateau Have Continuously Advanced From 1982 to 2011." *Proceedings of the National Academy of Sciences of the United States of America* 110, no. 11: 4309–4314. https://doi.org/10.1073/pnas.1210423110.

Zhang, X., Y. Yang, S. Piao, et al. 2015. "Ecological Change on the Tibetan Plateau." *Chinese Science Bulletin* 60, no. 32: 3048–3056.

Zhang, Y., S. Hong, D. Liu, and S. Piao. 2023. "Susceptibility of Vegetation Low-Growth to Climate Extremes on Tibetan Plateau." *Agricultural and Forest Meteorology* 331: 109323. https://doi.org/10.1016/j.agrformet.2023.109323.

Zhou, G., H. Ren, T. Liu, et al. 2023. "A New Regional Vegetation Mapping Method Based on Terrain-Climate-Remote Sensing and Its Application on the Qinghai-Xizang Plateau." *Science China Earth Sciences* 66, no. 2: 237–246. https://doi.org/10.1007/s11430-022-1006-1.

Zhu, Q., H. Chen, C. Peng, et al. 2023. "An Early Warning Signal for Grassland Degradation on the Qinghai-Tibetan Plateau." *Nature Communications* 14, no. 1: 6406. https://doi.org/10.1038/s41467-023-42099-4.

Supporting Information

Additional supporting information can be found online in the Supporting Information section.